J Am Oil Chem Soc (2011) 88:2035–2045
DOI 10.1007/s11746-011-1864-2

ORIGINAL PAPER

Insight into β-Carotene Thermal Degradation in Oils with Multiresponse Modeling

**Nawel Achir · Caroline Pénicaud · Sylvie Avallone ·
Philippe Bohuon**

Received: 13 January 2011 / Revised: 22 April 2011 / Accepted: 22 May 2011 / Published online: 12 June 2011

Abstract The aim of this study was to gain further insight into β-carotene thermal degradation in oils. Multiresponse modeling was applied to experimental high-performance liquid chromatography–diode array detection (HPLC–DAD) data (*trans*-, 13-*cis*-, and 9-*cis*-β-carotene concentrations) during the heat treatments (120–180 °C) of two β-carotene-enriched oils, i.e., palm olein and copra. The test of different reaction schemes showed that β-carotene isomerization reactions were dominant and reversible. The resulting *cis* isomers and *trans*-β-carotene simultaneously underwent oxidation and cleavage reactions at the same rate constant. From the kinetic analysis, it appeared that—contrary to oxidation and cleavage reactions—isomerization rate constants did not follow the Arrhenius law. However, the isomerization equilibrium constant increased with temperature, favoring isomer production, particularly 9-*cis*-β-carotene. Its production was shown to be concomitant with oxidation and cleavage reactions, indicating that 9-*cis*-β-carotene could be a good degradation indicator during oil storage or processing.

Keywords Carotenoid · Isomerization · 13-*cis*-β-carotene · 9-*cis*-β-carotene · Oxidation · Reaction scheme · Kinetics · Lipids

---

N. Achir (✉) · C. Pénicaud · P. Bohuon
UMR 95 QualiSud, TA B-95/16, 73 Av. J.F. Breton,
34398 Montpellier Cedex 5, France
e-mail: nawel.achir@cirad.fr

S. Avallone
UMR 204 NutriPass, 911 Avenue Agropolis,
34394 Montpellier Cedex 5, France

Introduction

β-carotene is the most widespread carotenoid and is found in a high content in orange vegetables, such as pumpkin, carrot, sweet potatoes, and palm fruit [1, 2]. With its perfect vitamin A dimer structure, β-carotene is the most important source of this vitamin. Its conjugated polyenic system is also responsible for its orange color, but, above all, for its antioxidant properties. β-carotene is a very efficient O_2 singlet quencher and can protect molecules against oxidation [3]. However, its unsaturated structure is very fragile and can degrade via two main reactions: isomerization and oxidation [4]. β-carotene isomerization involves a configuration change from its natural *trans* form to various *cis* isomer species. Double bonding is weakened by resonance, even at ambient temperature, thus, facilitating this interconversion [5]. However, isomerization was shown to be favored by temperature and, to a minor extent, by light [6]. The resulting isomers can still be converted into vitamin A, but with a lower yield [7]. Oxidation is the major cause of β-carotene loss and takes place through a radicalar mechanism. Indeed, the long double bond chain is an excellent substrate for free radical attack. These autooxidation reactions have high activation energies [8] and are irreversible, as the resulting products are oxicarotenoids and cleavage products such as apocarotenals and apocarotenones [9]. Hundreds of molecules can be produced from β-carotene, some of which are likely prooxidants [10]. The numerous reactions involved are strongly influenced by exterior conditions (i.e., temperature, oxygen pressure) and the medium composition [11].

Many studies have aimed at monitoring β-carotene degradation kinetics in order to control, predict, and optimize its retention during food storage. This dynamic approach is interesting for identifying major degradation pathways and their evolution as a function of exterior conditions, but most kinetic models described in the literature only represent β-carotene loss [12, 13]. These models may help in predicting β-carotene loss in comparable conditions but cannot indicate the prevalence of each degradation pathway, since a single apparent degradation rate constant includes all specific degradation rates. Some studies have not only monitored β-carotene loss but also degradation products, such as *cis* isomers [14], and, less frequently, oxidized or cleavage products [15]. However, no kinetic models were developed on the basis of these experiments. This is probably because the consideration of different degradation molecules requires knowledge of the degradation reaction scheme and the use of multiresponse modeling to identify the different reaction rate constants. This approach could still give insight into the reaction, as was the case for Maillard reactions in the study of van Boekel [16]. Surprisingly, very little work has been done on β-carotene with multiresponse modeling, whereas β-carotene degradation forms a very dense reaction scheme, the mechanisms of which are still very unclear [11]. Zepka et al. [17] proposed a simplified multiresponse model to represent carotenoid degradation in a model cashew apple juice. The reaction scheme involved parallel reactions of both *trans*-β-cryptoxanthin and *trans*-β-carotene to yield degradation compounds and mono-*cis* isomers. Therefore, through the global monitoring of the two types of product (volatile and non-volatile, respectively), they could identify the different rate constants, differentiate the two pathways, and even evaluate the temperature effect. However, specific studies on β-carotene degradation mechanisms could not be found. For instance, the very early stages of β-carotene autooxidation are not yet clear. Mordi [18] supposed that isomerization could be the first step of oxidation, whereas Mohamed et al. [19] suggested that oxidation could more easily occur directly on *trans*-β-carotene at its β-ring. Concerning the kinetic aspect, the main β-carotene isomerization rate constants are only available at low temperature when oxidative reactions are negligible [20]. Therefore, the influence of temperature, which can affect the reaction dynamics and, thus, change the main reaction pathways, has not yet been studied. *cis* isomer concentrations can be easily determined using reliable high-performance liquid chromatography (HPLC) devices developed for this purpose [21]. However, oxidized and cleavage molecules are much harder to monitor because of their high number due to random oxygen attack and their variable properties (different functions, volatility, etc.).

The aim of this study was to apply multiresponse modeling to the experimental data of β-carotene thermal degradation, along with high-performance liquid chromatography–diode array detection (HPLC–DAD) analysis in two frying oils at temperatures ranging from 120 to 180 °C. Firstly, simplified reaction schemes are proposed on the basis of the analysis of *trans*-β-carotene and its *cis* isomer concentrations during heat treatments. The focus was placed on the reversibility or not of the isomerization reactions and on their relationship with the formation of oxidized products. For each system, the rate constants were estimated by non-linear regression, via multiresponse modeling. After the election of the best scheme, the effect of temperature and oil type on the distinct reaction constants of isomerization and oxidation are discussed.

Materials and Methods

Thermal Treatment of β-Carotene-Enriched Oils

The experimental procedure used to collect experimental data was presented in a previous paper [22]. Briefly, thermal treatments were carried out on two commercial oils, i.e., palm olein and copra fat, previously enriched in β-carotene at an average concentration of 220 mg kg^{-1}, which is close to that found in red palm oil [23]. The isothermal treatment was achieved by using a small quantity of oil (1 mL) in vials placed in an instrumented reaction block providing high thermal homogeneity. The whole experimental device was covered with aluminum foil to prevent β-carotene degradation by light. The thermal degradation kinetics experiments were performed in duplicate with six points at four temperatures: 120 °C, 140 °C, 160 °C, and 180 °C. The 160 °C experiment was carried out in triplicate and the variation coefficients were extrapolated to other temperatures.

Determination of Isomers and Oxidized and Cleavage Concentrations

Trans- and *cis*-β-carotene analysis was done with an HPLC–DAD method adapted from Kimura and Rodriguez-Amaya [24] and de Sá and Rodriguez-Amaya [25] with a polymeric YMC-30 column (YMC Inc., Wilmington, NC, USA) in isocratic conditions [26].

All isomers were analyzed. Oxidized and cleavage products were evaluated by the following mass balance:

$$\text{Oxidation and cleavage products } \mathrm{OCP}_{(t)} = \textit{Trans-}\beta\text{-carotene}_{t=0} - \sum \textit{cis}\,\text{isomer}_{(t)} \quad (1)$$

Kinetic Modeling

Carotene change was described by a first-order kinetics equation:

$$\frac{\mathrm{d}[\mathrm{X}]}{\mathrm{d}t} = -k[X] \quad (2)$$

where X represents *trans*-β-carotene or a *cis* isomer, $[X]$ the concentration in mol l^{-1}, t the time (min), and k the reaction rate constant (min^{-1}).

Observable reaction schemes were drawn up according to the experimental findings. Once a reaction scheme was determined, it was translated into a system of four differential equations (one per compound, i.e., *trans*-β-carotene, 9-*cis* isomer, 13-*cis* isomer, and oxidation and cleavage products).

The reaction rate constants of this system of four differential equations were iteratively adjusted to the goodness of fit merit function with the Levenberg–Marquardt minimization procedure [27] using MATLAB® software (The MathWorks, Inc., Natick, MA, USA). This merit function was the root mean square error (RMSE) between experimental ($[X_{\mathrm{exp}}]$) and calculated ($[X_{\mathrm{pred}}]$) concentrations:

$$\mathrm{RMSE} = \sqrt{\frac{1}{n-1}\sum_{i=1}^{n}([X_{\mathrm{pred}}] - [X_{\mathrm{exp}}])^2} \quad (3)$$

where n is the number of data.

Reaction rate constants were identified independently for each temperature studied.

A stochastic method was used to evaluate the uncertainty of the identified parameters. The standard deviations of identified rate constants were determined via Monte Carlo simulations [28]. In order to simulate virtual data, a random scatter was added to each data point $[X_{\mathrm{exp}}]$:

$$[\tilde{X}] = [X_{\mathrm{exp}}] + U_x\delta \quad (4)$$

with $[\tilde{X}]$ being the virtual data generated (carotene concentrations), $[X_{\mathrm{exp}}]$ the real measured value, U_{x} the estimated error on the measured value, and δ a random number whose elements are normally distributed with mean 0 and variance 1. The estimated error considered for each carotene was calculated from the variation coefficients obtained from the experiment at 160 °C, which was carried out in triplicate.

These normally distributed random errors were considered to be independent (thus, their covariance was zero). However, each set of generated data included joint effects of errors on all carotenes, since the identifications were done considering all of the experimental results for each temperature. These virtual data were generated with MATLAB® software (The MathWorks, Inc., Natick, MA, USA).

For a given operating condition, $m = 1{,}000$ datasets were randomly drawn using adequate equation(s) and the m values of parameters to be determined were identified as described above on m separate datasets. The standard deviation was estimated for each rate constant from the m values.

Model Discrimination

To discriminate the proposed models, the residual sum of squares (RSS) and the Akaike information criterion (AIC) were compared. The RSS is expressed as follows:

$$\mathrm{RSS} = \sum_{i=1}^{n}([X_{\mathrm{optipred}}] - [X_{\mathrm{exp}}])^2 \quad (5)$$

where n is the number of data points, $[X_{\mathrm{exp}}]$ the experimental result, and $[X_{\mathrm{optipred}}]$ the optimized simulated result.

The RSS is a measure of the discrepancy between the experimental and simulated data. A small RSS indicates a good fit of the model to the data.

The AIC is a complementary measure of goodness of fit used by van Boekel [16]. It describes the trade-off between the accuracy (RSS) and complexity of the model (number of parameters). It is expressed as follows:

$$\mathrm{AIC} = n\ln\left(\frac{\mathrm{RSS}}{n}\right)^2 + 2(p+1) \quad (6)$$

where n is the number of data points and p the number of estimated parameters.

A small AIC indicates that the model has a good fit to the experimental data with a limited number of parameters.

Influence of Temperature

The rate constants k were assumed to vary with the absolute temperature T (K) according to the Arrhenius law:

$$k = k_0 \exp\left(\frac{-E_{\mathrm{a}}}{RT}\right) \quad (7)$$

where k_0, E_{a}, T, and R are the pre-exponential factor (min^{-1}), the activation energy (J mol^{-1}), the oil temperature (K), and the gas constant (8.314 J mol^{-1} K^{-1}), respectively. Because of the close correlation between k_0 and E_{a}, a simple reparametering was achieved by introducing a reference temperature as follows:

$$k = k_{\mathrm{ref}} \exp\left(\frac{-E_{\mathrm{a}}}{R}\left(\frac{1}{T} - \frac{1}{T_{\mathrm{ref}}}\right)\right) \quad (8)$$

In this reparametering, the pre-exponential factor k_{ref} becomes the rate constant at the reference temperature chosen in the middle of the studied temperature range, i.e., 150 °C.

Statistical Analysis

A principal component analysis was done with XLSTAT® (Addinsoft, Paris, France).

Results and Discussion

Description of Experimental Results

Figure 1 shows the experimental data for *trans*-β-carotene (all-E) thermal degradation in palm olein (a–d) and in copra (e–h) at four oil temperatures, 120, 140, 160, and 180 °C. The reduced concentrations $\frac{[X]}{[\text{all - }E]_0}$ are presented at different heating time intervals t, where $[X]$ is the carotene form (*trans* or *cis*) concentration and $[\text{all-}E]_0$ is the initial concentration of *trans*-β-carotene in the vials. Figure 1a and e present variations in the reduced concentration of *trans*-β-carotene, while Fig. 1b, c and f, g show the reduced concentrations of the major *cis* isomers identified during the heat treatment, i.e., 13-*cis* (13-Z) and 9-*cis*-β-carotene (9-Z), respectively. Finally, Fig. 1d and h present the oxidized or cleaved products of β-carotene calculated by the mass balance according to Eq. 1.

The experimental results presented in Fig. 1 were presented in a previous paper [22]. In both oils, the decrease in *trans*-β-carotene (Fig. 1a, e) was concomitant to the formation of isomers (Fig. 1b, c and f, g) and oxidized and cleavage products (Fig. 1d, h). Therefore, isomerization, oxidation, and cleavage were simultaneous reactions that may be interlinked, as suggested by Mordi [18]. The main isomers identified were 13-*cis*- and 9-*cis*-β-carotene. This result is consistent with the β-carotene isomers most often identified after heat treatment [14, 29, 30]. Mohamed et al. [19] also showed via molecular modeling that, among *cis* isomers, the lowest energy configurations were 9-*cis*- and 13-*cis*-β-carotene. Their initial production rate was very high, suggesting that they could be primary degradation products of *trans*-β-carotene. There was a relatively high amount of *cis* isomers in both oils: the average maximum sum of isomers was 30–40%. This amount was even higher at lower temperatures in copra fat. In comparison, during the heat treatment of carrot juice, Marx et al. [30] found only 13 and 3% of 13-*cis*- and 9-*cis*-β-carotene, respectively, after 60 min at 100 °C. Dhuique-Mayer et al. [31] did not identify any β-carotene isomers, whereas they noted a similar *trans*-β-carotene degradation rate during the heat treatment of citrus juice. Chen and Huang [6] stated that the β-carotene isomerization level was dependent on the solvent and that higher levels were reached in non-polar solvents. The high *cis* isomer concentration may have been due to the hydrophobic properties of the oils.

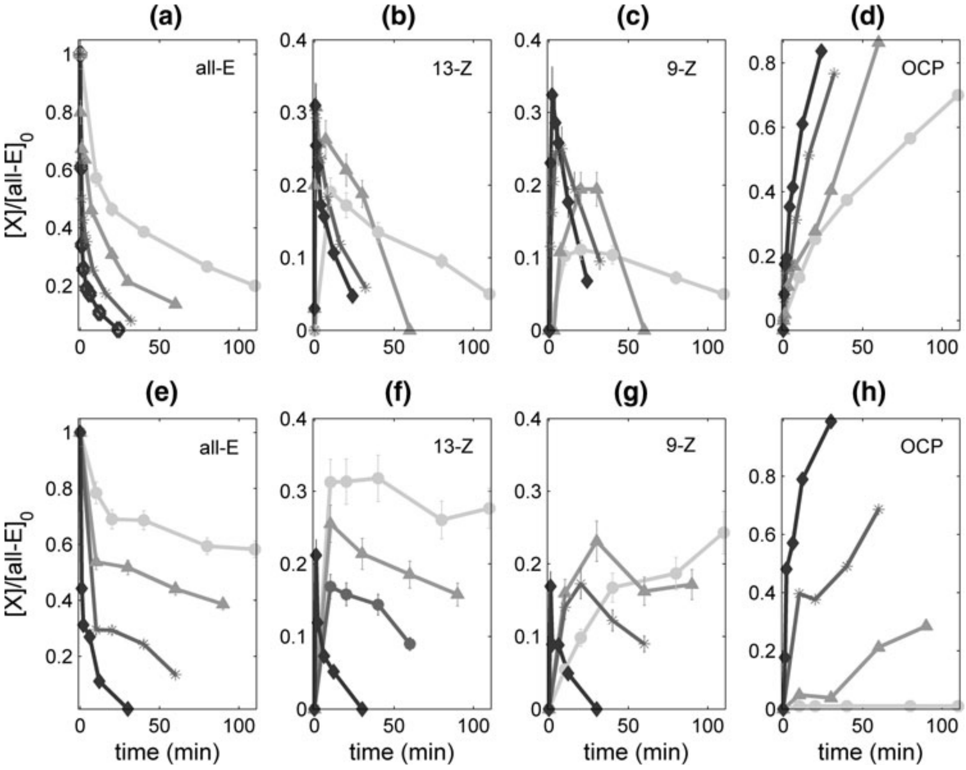

Fig. 1 Experimental reduced concentration of *trans*-β-carotene (all-E), 13-*cis*- (*13-Z*), and 9-*cis*-β-carotene (*9-Z*) during heat treatments at four oil temperatures (*filed circles* 120, *filled triangles* 140, *asterisks* 160, and *filled diamonds* 180 °C) in palm olein (**a**–**c**) and copra (**e**–**g**). The *error bars* represent the standard deviation ($n = 3$). The concentration of oxidized and cleavage products (*OCP*) was calculated by the mass balance (Eq. 1) in palm olein (**d**) and copra (**h**)

Maximum 9-*cis*-β-carotene concentrations were reached after those of 13-*cis*-β-carotene, suggesting that 9-*cis*-β-carotene was produced after 13-*cis*-β-carotene. This phenomenon has been observed in many other studies, suggesting that 9-*cis*-β-carotene is produced under more severe treatment [14, 30]. Like *trans*-β-carotene, 13-*cis*- and 9-*cis*-β-carotene also underwent oxidation and cleavage degradation as their concentrations decreased as a function of the heating time. Besides, their concentrations dropped to zero at the end of some experiments. They could, therefore, be considered as intermediary compounds. The oxidized and cleavage product concentrations were nil at $t = 0$, but they kept increasing as a function of the heating time, so they could be considered as secondary products. This indicated that the dynamics of isomerization and oxidation/cleavage reactions differed markedly. Note that, at 120 °C in copra (Fig. 1e–h), only the isomerization of *trans*-β-carotene took place at the chosen time scale. This indicated that isomerization required less energy in comparison to oxidation and cleavage reactions. Oxidation and cleavage reactions occurred at 120 °C in palm olein. This could have been due to the more unsaturated nature of this oil in comparison to hydrogenated copra fat and to the possible oxidation of fatty acids.

Proposal of Simplified and Observable Reaction Schemes

From the previous experimental observations, a first simplified and observable scheme is proposed in Fig. 2 (scheme 1). The main assumptions for building this model were the conversion of *trans*-β-carotene (all-*E*) into its major *cis* isomers (13-*cis*- and 9-*cis*-β-carotene) and oxidation and cleavage products (OCP) at rate constants k_1, k_2, and k_3, respectively. 13-*cis*- and 9-*cis*-β-carotene were also assumed to give rise to OCP with rate constants k_4 and k_5, respectively.

The corresponding set of ordinary differential equations for the first reaction scheme is:

$$\frac{\mathrm{d}[\mathrm{allE}]}{\mathrm{d}t} = -(k_1 + k_2 + k_3)[\mathrm{all}E] \tag{9}$$

$$\frac{\mathrm{d}[13\mathrm{Z}]}{\mathrm{d}t} = k_1[\mathrm{all}E] - k_4[13Z] \tag{10}$$

$$\frac{\mathrm{d}[9\mathrm{Z}]}{\mathrm{d}t} = k_2[\mathrm{all}E] - k_5[9Z] \tag{11}$$

$$\frac{\mathrm{d}[\mathrm{OCP}]}{\mathrm{d}t} = k_3[\mathrm{all}E] + k_4[13Z] + k_5[9Z] \tag{12}$$

The results of the experimental data fit are presented in Fig. 3, scheme 1. A poor experimental data fit was obtained, especially for *trans*-β-carotene and 13-*cis*-β-carotene, whose concentrations were underestimated. In addition, concentrations of oxidized and cleavage products were overevaluated. The negative constant of *trans*-β-carotene obtained in this first scheme could indicate that this compound may be "formed" during its degradation. This phenomenon could be possible, providing that there is a back-isomerization reaction. This is a realistic assumption since, experimentally, 13-*cis*- and 9-*cis*-β-carotene maximums seemed to be constrained. For both isomers, no more than 30% were produced and, as stated earlier, the sum of isomers did not exceed 40%. This fact suggests a possible equilibrium in the isomerization reactions. In addition, the repeatability of the *trans*-β-carotene analysis was better than that of *cis* isomers (variation coefficient of 5% as compared to 10–15%). This highlights the instability of isomers that could be involved in both cleavage and back-isomerization. Molnár [20] showed, in experiments involving isomers of zeaxanthin in benzene, that isomerization is a reversible reaction. Moreover, other studies have showed that, generally, 9-*cis*- and 13-*cis*-β-carotene could not convert to each other [32].

In the second reaction scheme, the back-isomerization of both 13-*cis*- and 9-*cis*-β-carotene to *trans*-β-carotene is considered with the new rate constants k_3 and k_4. To simplify the model, only one oxidation and cleavage constant, k_5, was employed for *trans*-, 13-*cis*-, and 9-*cis*-β-carotene (Fig. 2, scheme 2). Indeed, the same model with different oxidation and cleavage constants exhibited results that were not any better (not shown here). The corresponding system of differential equations is presented below:

$$\frac{\mathrm{d}[\mathrm{allE}]}{\mathrm{d}t} = -(k_1 + k_2 + k_5)[\mathrm{all}E] + k_3[13Z] + k_4[9Z] \tag{13}$$

$$\frac{\mathrm{d}[13\mathrm{Z}]}{\mathrm{d}t} = k_1[\mathrm{all}E] - (k_3 + k_5)[13Z] \tag{14}$$

$$\frac{\mathrm{d}[9\mathrm{Z}]}{\mathrm{d}t} = k_2[\mathrm{all}E] - (k_4 + k_5)[9Z] \tag{15}$$

$$\frac{\mathrm{d}[\mathrm{OCP}]}{\mathrm{d}t} = k_5([\mathrm{all}E] + [13Z] + [9Z]) \tag{16}$$

Model 2, with the same number of constants as model 1, was found to be much more adapted. The experimental data fit was very good, as shown in Fig. 3. With respective values of 0.033 and −459, the RSS (Eq. 5) and the AIC (Eq. 6) were better (i.e., lower) than those found for model 1 (0.365 and −296, respectively). Back-isomerization, thus, seemed to be a reliable assumption. This model also showed that a single oxidation and cleavage constant for *trans* and *cis* isomers was suitable. Therefore, *trans* and *cis* isomers were equally sensitive to oxidation and cleavage. This is out of line with some assumptions of higher degradation of *cis* isomers [18].

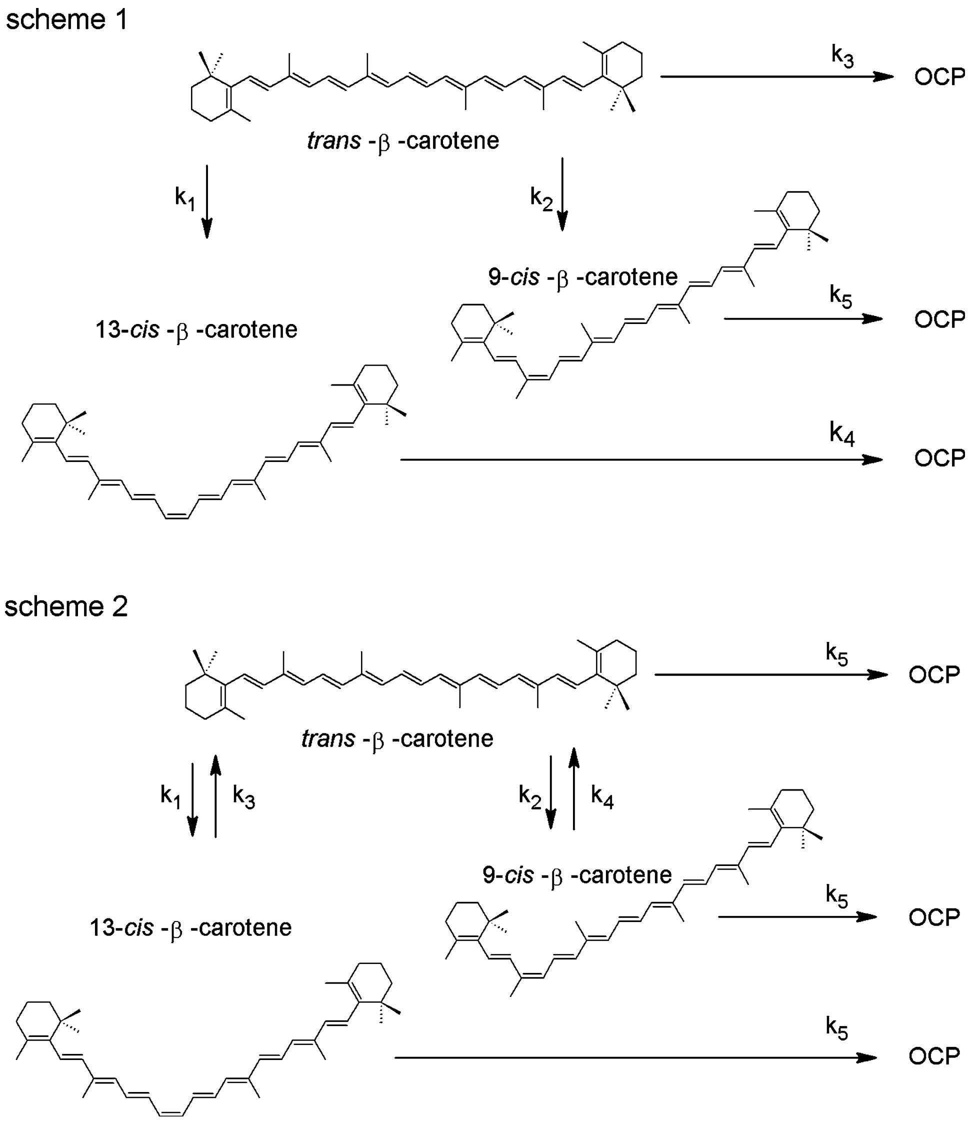

Fig. 2 Observable reaction schemes for the thermal degradation of *trans-β*-carotene in oils

The aim of the following section was to test the robustness of model 2 for different oil temperatures and types, and to consider their effects on the kinetic constants of isomerization and oxidation/cleavage reactions.

Effect of Experimental Conditions of Kinetic Parameters on Identified Rate Constants from Model 2

On the basis of model 2, reaction constants were identified from the experimental data of Fig. 1, obtained in the two oils, i.e., palm olein and copra, at four temperatures, ranging from 120 to 180 °C. The corresponding rate constants are presented in Table 1. Moreover, the RSS (Eq. 5) and the AIC (Eq. 6) are presented in order to evaluate the goodness of fit. The resulting simulated data are illustrated in Fig. 4 for the extreme temperatures of the studied domain, i.e., 120 and 180 °C. This figure shows that the experimental data fit was good for both oils. Besides, the RSS values obtained for each oil and each temperature were lower than the 0.365 value obtained with model 1 (Fig. 3). This indicated that the model was robust and could successfully predict the contents of carotenes and oxidation products in the temperature range studied and for both oils. This was confirmed by the low AIC values, ranging from −192 to −491. The AIC is sensitive to the number of experimental data, *n* (Eq. 6). For the same RSS value, the AIC value decreases as the number of data points increases, and the better the model fits. Indeed, the higher number of points represented well by a model, the better is the model. As shown in Table 1, the number of data points *n* was lower for experiments conducted in copra fat. Therefore, the resulting AIC values were higher than those obtained in palm olein. The highest AIC value of −192 was obtained at 160 °C, which also corresponded to the highest RSS value of 0.121.

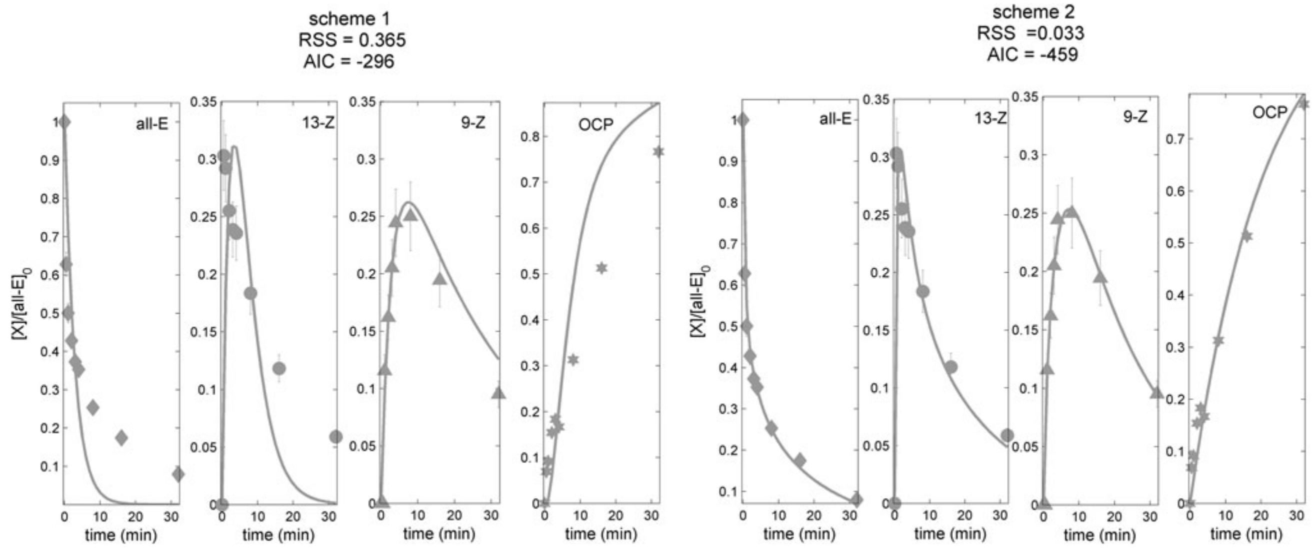

Fig. 3 Model fit (*lines*) to experimental data (*dots*) of the thermal degradation of *trans*-β-carotene for schemes 1 and 2 presented in Fig. 2. Experimental data were obtained in palm olein at 160 °C

Table 1 Identified kinetic constants obtained from the model fit

Oil	Temperature (°C)	Reaction rate constants (min^{-1})					Model goodness evaluation		
		k_1	k_2	k_3	k_4	k_5	RSS	n	AIC
Palm olein	120	0.063 ± 0.010	0.021 ± 0.002	0.185 ± 0.031	0.077 ± 0.012	0.011 ± 0.001	0.008	24	−371
	140	0.568 ± 0.163	0.033 ± 0.003	0.939 ± 0.315	0.038 ± 0.005	0.025 ± 0.002	0.074	32	−376
	160	0.824 ± 0.190	0.178 ± 0.022	1.259 ± 0.325	0.152 ± 0.036	0.047 ± 0.060	0.033	36	−491
	180	0.779 ± 0.156	0.396 ± 0.049	1.095 ± 0.260	0.296 ± 0.060	0.089 ± 0.011	0.082	32	−370
Copra	120	0.141 ± 0.015	0.042 ± 0.002	0.269 ± 0.032	0.128 ± 0.008	0.000 ± 0.000	0.055	24	−280
	140	0.106 ± 0.012	0.037 ± 0.007	0.239 ± 0.026	0.082 ± 0.019	0.004 ± 0.001	0.008	20	−300
	160	0.045 ± 0.014	0.039 ± 0.007	0.078 ± 0.036	0.069 ± 0.020	0.020 ± 0.002	0.121	20	−192
	180	0.556 ± 0.127	0.394 ± 0.117	1.366 ± 0.463	1.141 ± 0.424	0.168 ± 0.112	0.079	24	−263

The standard deviations were obtained by Monte Carlo simulations

Globally, in both oils, the rate constants increased as a function of temperature. The only exception was in copra fat at 160 °C, where the rate constants were significantly lower than those obtained at 140 °C. However, as stated earlier, the worst model fit was obtained for this temperature. This was possibly due to experimental bias in this set of experiments.

Influence of Temperature on Isomerization and Back-Isomerization Rate Constants

Generally, the rate constants obtained for the isomerization reactions were much higher than those obtained for the reaction and cleavage reactions. Indeed, with values ranging from 0 to 0.168 min^{-1}, the rate constant k_5 always exhibited the lowest value for each experiment. Conversely, the rate constants of isomerization and back-isomerization were never nil and, sometimes, were over 1 min^{-1} (Table 1). This indicates that isomerization and back-isomerization are very highly dynamic reactions in oils. For both oils, the highest rate constant values were obtained for k_1 and k_3, which were related to 13-*cis*-β-carotene. Indeed, k_1 and k_3 reached maximums of 0.824 and 1.259 min^{-1} at 160 °C in palm olein and 0.556 and 1.366 min^{-1} at 180 °C in copra fat. Those results explain the overall higher amount of 13-*cis*-β-carotene (Figs. 1 and 4). This configuration, thus, seemed to be favored.

Globally, when the oil temperature increased, the rate constant of production of a *cis* isomer increased at the same order of magnitude as its rate of back-isomerization to *trans*-β-carotene (Table 1). Therefore, k_1 and k_3 and k_2 and k_4 (cf. Scheme 2) varied in the same manner. This reflected the equilibrium of the isomerization reactions. Regarding their values, k_1 and k_3 and k_2 and k_4 obviously did not

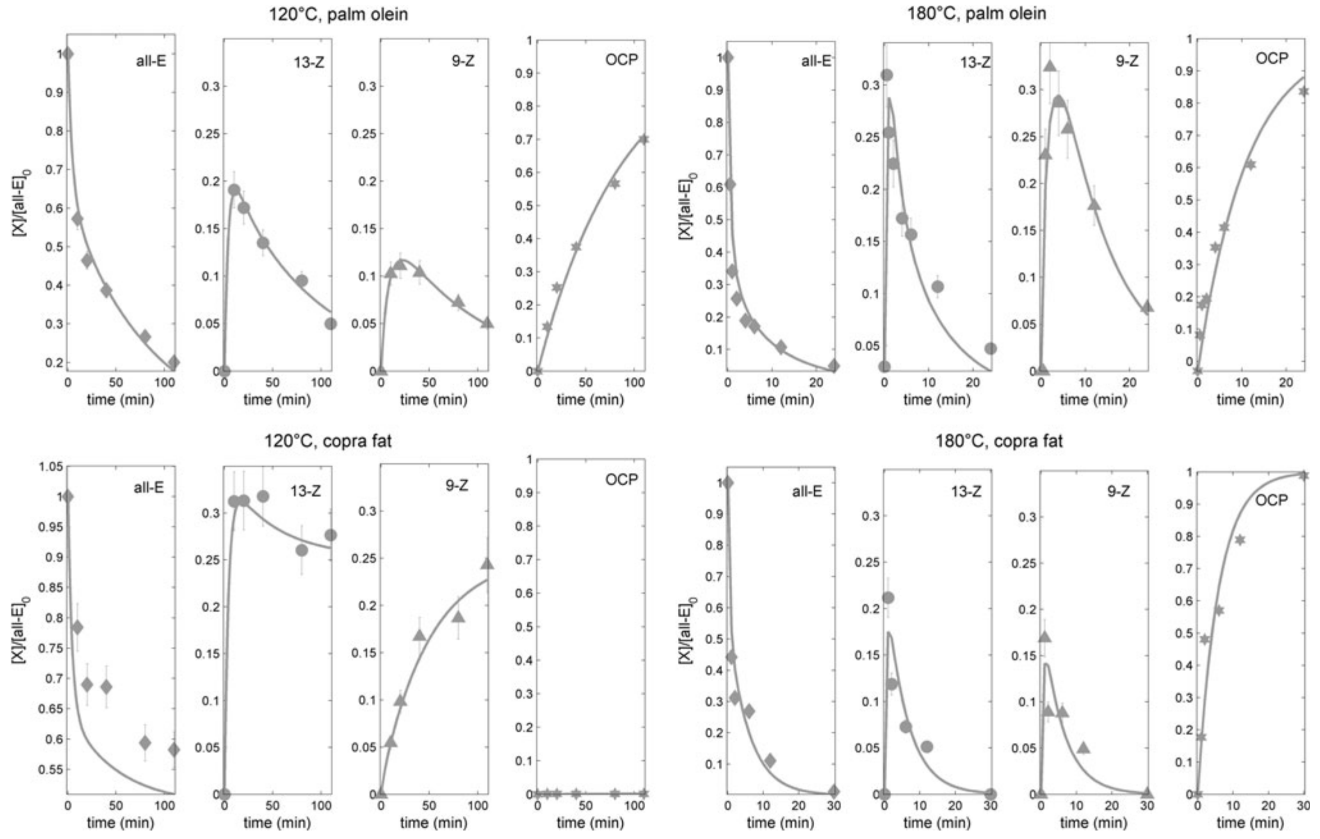

Fig. 4 Model fit (*lines*) to experimental data (*dots*) of the thermal degradation of *trans*-β-carotene (all-*E*). Experimental data were obtained in palm olein at (**a**) 120 and (**b**) 180 °C or in copra at (**c**) 120 and (**d**) 180 °C

follow the Arrhenius law. For instance, in palm olein, k_1 and k_3 exhibited a maximum at 160 °C and their value decreased at 180 °C. In copra fat, k_2 and k_4 stagnated from 120 to 160 °C and then sharply increased at 180 °C. However, a general pattern could be observed in their values. For both *cis* isomers, at low temperature, their production rate constant was lower than their rate of back-isomerization to the *trans* form. For instance, the production rate constants of 13-*cis*- and 9-*cis*-β-carotene in palm olein at 120 °C were 0.063 and 0.021 min^{-1}, respectively, as compared to the highest values of back-isomerization constants of 0.185 and 0.077 min^{-1}, respectively. The same pattern was observed in copra oil. At 120 °C, $k_1 = 0.141 < k_3 = 0.269$ and $k_2 = 0.042 < k_4 = 0.128$. However, in palm olein, when the temperature increased, the production rate increased markedly and sometimes surpassed the back-isomerization rate. For instance, at 180 °C, in the case of 9-*cis*-β-carotene, its production rate constant of 0.329 min^{-1} was higher than its back-isomerization value of 0.296 min^{-1}. This reflects a modification of the equilibrium constants of reactions K_{k_1/k_3} and K_{k_2/k_4} as a function of the temperature. Their patterns are presented in Fig. 5a, b. In palm olein, when the temperature increased, K_{k_1/k_3} and K_{k_2/k_4} also increased. Therefore, the reaction was equilibrated but the temperature favored the isomerization reaction. Indeed, from 120 to 180 °C, K_{k_1/k_3} increased from 0.34 to 0.71 and K_{k_2/k_4} from 0.27 to 1.34 (Fig. 5a, b). For both isomers, the corresponding curves reached a horizontal asymptote, which was <1 for K_{k_1/k_3} and >1 for K_{k_2/k_4}. Thus, from 160 °C, the *trans*- to 9-*cis*-β-carotene reaction was dominant. This could explain why 9-*cis*-β-carotene was more dominant under more severe heat treatments. In the case of copra oil, no significant variations in K_{k_1/k_3} and K_{k_2/k_4} as a function of temperature were observed. In addition, the simulated data at 160 °C were hampered by uncertainty. The influence of temperature on the isomerization equilibria was, therefore, not as clear as it was for palm olein. Nevertheless, in that oil, irrespective of the temperature, K_{k_1/k_3} and K_{k_2/k_4} values of less than 1 implied a dominant reaction from *cis* isomers to the *trans* form.

Influence of Temperature on the Oxidation and Cleavage Constant

Contrary to isomerization, the oxidation and cleavage reactions are not equilibrated, but they are irreversible reactions. In both oils, the influence of temperature on the

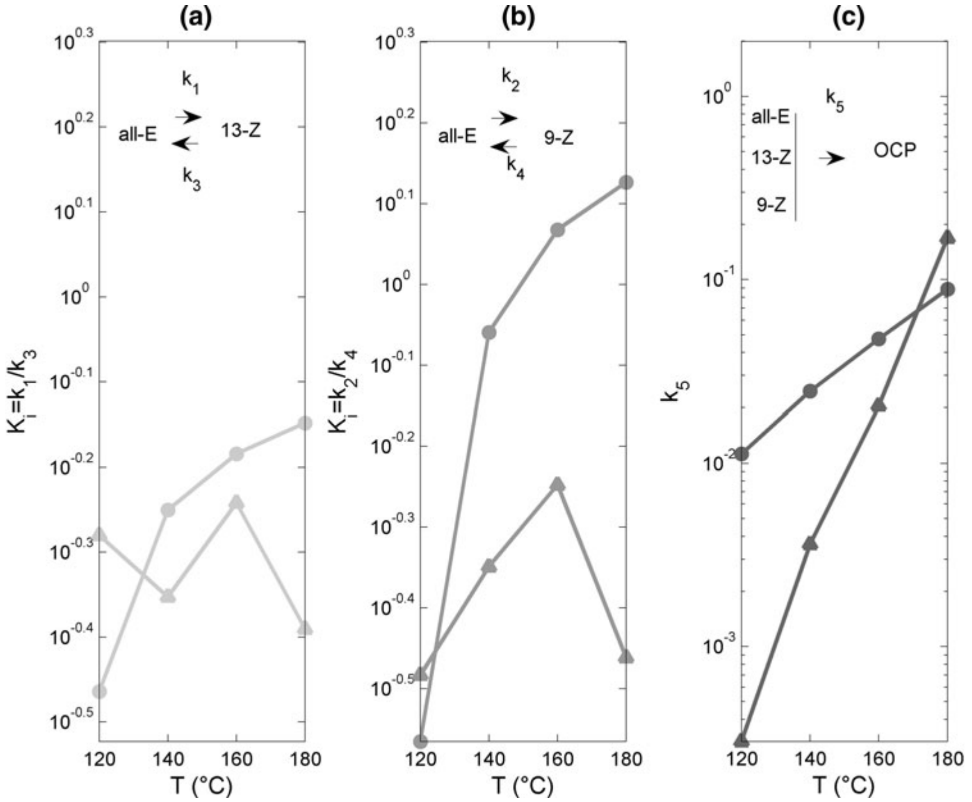

Fig. 5 Variations in equilibrium constants (log scale) of (**a**) *trans*-β-carotene isomerization in 13-*cis*-β-carotene (k_1/k_3), (**b**) in 9-*cis*-β-carotene (k_2/k_4), and (**c**) oxidation/cleavage constant (k_5) as a function of temperature in palm olein (*filled circles*) and copra (*filled triangles*)

oxidation and cleavage rate constant k_5 was marked. k_5 values followed the Arrhenius law (Eq. 7) as they increased exponentially as a function of the oil temperature (Fig. 5c). Experimentally, the increase in k_5 was closely linked to the decoloration of the oils. For instance, in copra fat, at 120 °C, while k_5 was nil, the absorbance at 450 nm of the oil barely decreased during the 120-min experiment. Indeed, *cis* isomers also absorbed light at 450 nm. On the contrary, at 180 °C, while $k_5 = 0.168\ \text{min}^{-1}$, almost total decoloration was observed within the first 10 min. This color change was due to the cleavage of β-carotene, giving rise to smaller compounds whose absorbance maxima were much less than 450 nm. As no oxidation products were found in the oils, these products likely have a very small life expectancy and, once produced, cleavage products would be immediately formed. Therefore, the choice of one apparent oxidation/cleavage constant was warranted.

By using the k_5 values (Table 1) in Eq. 8, the activation energy of oxidation/cleavage reactions were calculated and were equal to 51 kJ mol^{-1} ($R^2 = 0.99$), with a $k_{5\text{ref}}$ of 3.4×10^{-2} min^{-1} for palm olein and 171 kJ mol^{-1} ($R^2 = 0.99$) and $k_{5\text{ref}} = 6.8 \times 10^{-3}$ min^{-1} for copra fat. Therefore, the influence of temperature on the k_5 values differed markedly as a function of the oil type. Indeed, in copra, temperature had a more substantial influence. For instance, with values of 0 to 0.02 min^{-1}, k_5 was inferior in this fat in comparison to the values of 0.01 to 0.04 min^{-1} in palm olein from 120 to 160 °C. However, k_5 became twofold superior in copra at 180 °C (0.168 min^{-1} compared to 0.089 min^{-1}). Therefore, oxidation and cleavage reaction rate constants were globally higher in palm olein but less sensitive to temperature than in copra. These differences could be attributed to differences in oil composition in terms of their fatty acid contents. Indeed, palm olein contains unsaturated fatty acids, which are more prone to oxidation than those of copra, which may explain the oxidation and cleavage reactions which occurred at 120 °C. On the other hand, there could be competition between unsaturated lipids and β-carotene as oxidation substrates, which would limit the decrease in β-carotene. This phenomenon was observed by Rossi et al. [33] in the case of vitamin E degradation in oils.

Relationship Between Isomerization and Cleavage Reactions

To analyze the correlation between kinetic constants, a principal component analysis (PCA) was carried out using the kinetic constant values of Table 1, i.e., from palm olein and copra fat. The results are shown in Fig. 6. Only two principal components (factors 1 and 2) were necessary to account for 96% of the total variance. Temperature was the

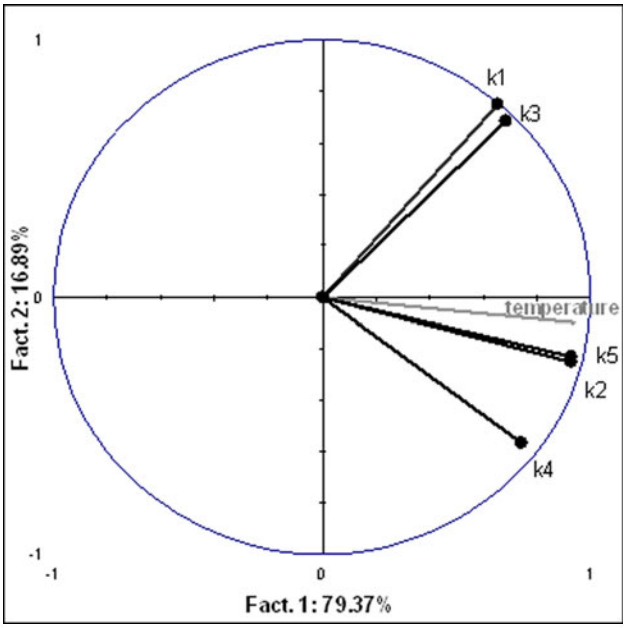

Fig. 6 Projection circle of kinetic constant variables obtained by principal component analysis (PCA) and from the numerical data of Table 1

dominant feature in the first principal component, accounting for 79.37% of the total variability. The main conclusions are that all constants were correlated with temperature but the isomerization reaction constant k_2 (*trans*- to 9-*cis*-*β*-carotene) and the oxidation/cleavage constant were the most sensitive to a temperature change. Constants k_1 and k_3 were closely correlated, i.e., when isomerization to 13-*cis*-*β*-carotene increased, the back-isomerization of 13-*cis*-*β*-carotene into the *trans* form concomitantly increased. The other reaction constants relative to 9-*cis*-*β*-carotene, k_2 and k_4, were also correlated with each other. Temperature, therefore, increased the dynamics of change from *trans* to *cis* and *cis* to *trans* configurations. Interestingly, k_5, the oxidative and cleavage constant, was closely correlated with the k_2 constant. Several authors have noticed that the 9-*cis* isomer appears under severe treatment conditions [14]. This was confirmed by our findings and, in addition, the 9-*cis*-*β*-carotene isomer appeared concomitantly to cleavage and to the intensification of oxidative reactions.

Conclusion

In this study, multiresponse modeling helped in choosing the most probable reaction scheme, which was the isomerization of *trans*-*β*-carotene into its principal isomers, i.e., 13-*cis*- and 9-*cis*-*β*-carotene, and the simultaneous back-isomerization of these isomers into the *trans* form. The best model also showed that *trans*-, 13-*cis*-, and 9-*cis*-*β*-carotene underwent oxidation and cleavage reactions at the same rate. Isomerization reactions of *β*-carotene in oils, therefore, involved a ceaseless backwards and forwards change in configuration, while the oxidation/cleavage reactions were irreversible. These reactions were all concomitant but very different in their nature and kinetics. Isomerization and back-isomerization reaction constants generally exhibited high values in oils. All constants increased with temperature. However, the temperature-dependency differed markedly for isomerization and for oxidation/cleavage reactions. For the latter reactions, the rate constants followed the Arrhenius law. The activation energy calculations revealed that these reactions could be activated very differently as a function of the oil composition. In the case of isomerization rate constants, the Arrhenius law was not suitable. However, when representing the equilibrium constant of these reactions, an increase in temperature clearly displaced the equilibrium of the reaction to the benefit of isomerization. The study of the relationship between all rate constants showed that isomerization and back-isomerization reactions were closely linked. In addition, the oxidation and cleavage constant was correlated with 9-*cis* isomer production. This was very interesting, since this latter isomer is easier to monitor than cleavage products and could be an indicator of oxidation/cleavage reactions during a process. This strategy, which will have to be confirmed in other oils, could be interesting to increase *β*-carotene retention during the storage of *β*-carotene-rich oils or during processing involving the heating of oils during oil refining or deep-fat frying.

References

1. Bhaskarachary K, Sankar Rao DS, Deosthale YG, Reddy V (1995) Carotene content of some common and less familiar foods of plant origin. Food Chem 54:189–193
2. Kim Y-N, Giraud DW, Driskell JA (2007) Tocopherol and carotenoid contents of selected Korean fruits and vegetables. J Food Compos Anal 20:458–465
3. Laguerre M, Lecomte J, Villeneuve P (2007) Evaluation of the ability of antioxidants to counteract lipid oxidation: existing methods, new trends and challenges. Prog Lipid Res 46:244–282
4. Rodríguez-Amaya DB (2001) A guide to carotenoid analysis in foods. OMNI Research, Washington, DC
5. Dugave C, Demange L (2003) *cis-trans* isomerization of organic molecules and biomolecules: implications and applications. Chem Rev 103:2475–2532
6. Chen BH, Huang JH (1998) Degradation and isomerization of chlorophyll a and [beta]-carotene as affected by various heating and illumination treatments. Food Chem 62:299–307
7. Thurnham DI (2007) Bioequivalence of *β*-carotene and retinol. J Sci Food Agr 87:13–39
8. Gurr MI, Harwood JL, Frayn KN (2002) Lipid biochemistry: an introduction. Blackwell, Oxford

9. Caris-Veyrat C, Amiot M-J, Ramasseul R, Marchon J-C (2001) Mild oxidative cleavage of beta,beta-carotene by dioxygen induced by a ruthenium porphyrin catalyst: characterization of products and of some possible intermediates. New J Chem 25:203–206
10. Subagio A, Morita N (2001) Instability of carotenoids is a reason for their promotion on lipid oxidation. Food Res Int 34:183–188
11. Pénicaud C, Achir N, Dhuique-Mayer C, Dornier M, Bohuon P (2011) Degradation of β-carotene during fruits and vegetables processing or storage: reaction mechanisms and kinetics aspects. Fruits (in press)
12. Koca N, Burdurlu HS, Karadeniz F (2007) Kinetics of colour changes in dehydrated carrots. J Food Eng 78:449–455
13. Ahmed J, Shivhare US, Sandhu KS (2002) Thermal degradation kinetics of carotenoids and visual color of papaya puree. J Food Sci 67:2692–2695
14. Hiranvarachat B, Suvarnakuta P, Devahastin S (2008) Isomerisation kinetics and antioxidant activities of [beta]-carotene in carrots undergoing different drying techniques and conditions. Food Chem 107:1538–1546
15. Bechoff A, Dhuique-Mayer C, Dornier M, Tomlins KI, Boulanger R, Dufour D, Westby A (2010) Relationship between the kinetics of [beta]-carotene degradation and formation of norisoprenoids in the storage of dried sweet potato chips. Food Chem 121:348–357
16. van Boekel MAJS (2008) Kinetic modeling of reactions in foods. CRC Press, Boca Raton, FL
17. Zepka LQ, Borsarelli CD, Pereira da Silva MAA, Mercadante AZ (2009) Thermal degradation kinetics of carotenoids in a cashew apple juice model and its impact on the system color. J Agric Food Chem 57:7841–7845
18. Mordi RC (1993) Mechanism of beta-carotene degradation. Biochem J 292:310–312
19. Mohamed N, Hashim R, Rahman NA, Zain SM (2001) An insight to the cleavage of [beta]-carotene to vitamin A: a molecular mechanics study. J Mol Struct Theochem 538:245–252
20. Molnár P (2009) Research of the (*E*/*Z*)-isomerization of carotenoids in Pécs since the 1970s. Arch Biochem Biophys 483:156–164
21. Sander LC, Sharpless KE, Craft NE, Wise SA (1995) Development of engineered stationary phases for the separation of carotenoid isomers. National Institute of Standards and Technology, Gaithersburg, MD
22. Achir N, Randrianatoandro VA, Bohuon P, Laffargue A, Avallone S (2010) Kinetic study of beta-carotene and lutein degradation in oils during heat treatment. Eur J Lipid Sci Technol 112:349–361
23. Sambanthamurthi R, Sundram K, Tan Y-A (2000) Chemistry and biochemistry of palm oil. Prog Lipid Res 39:507–558
24. Kimura M, Rodriguez-Amaya DB (2002) A scheme for obtaining standards and HPLC quantification of leafy vegetable carotenoids. Food Chem 78:389–398
25. de Sá MC, Rodriguez-Amaya DB (2003) Carotenoid composition of cooked green vegetables from restaurants. Food Chem 83:595–600
26. Qiu D, Chen Z-R, Li H-R (2009) Effect of heating on solid beta-carotene. Food Chem 112:344–349
27. Gill EP, Murray W, Wright MH (1981) Practical optimisation. Academic Press, New York
28. Hessler JP (1997) The use of Monte Carlo simulations to evaluate kinetic data and analytic approximations. Int J Chem Kinet 29:803–817
29. Chen JP, Tai CY, Chen BH (2007) Effects of different drying treatments on the stability of carotenoids in Taiwanese mango (*Mangifera indica* L.). Food Chem 100:1005–1010
30. Marx M, Stuparic M, Schieber A, Carle R (2003) Effects of thermal processing on *trans-cis*-isomerization of β-carotene in carrot juices and carotene-containing preparations. Food Chem 83:609–617
31. Dhuique-Mayer C, Tbatou M, Carail M, Caris-Veyrat C, Dornier M, Amiot MJ (2007) Thermal degradation of antioxidant micronutrients in citrus juice: kinetics and newly formed compounds. J Agric Food Chem 55:4209–4216
32. Pesek CA, Warthesen JJ (1990) Kinetic model for photoisomerization and concomitant photodegradation of beta-carotenes. J Agric Food Chem 38:1313–1315
33. Rossi M, Alamprese C, Ratti S (2007) Tocopherols and tocotrienols as free radical-scavengers in refined vegetable oils and their stability during deep-fat frying. Food Chem 102:812–817